AGU PUBLICATIONS

JGR

Journal of Geophysical Research: Oceans

RESEARCH ARTICLE

10.1002/2017JC012983

Key Points:

- The reversals in the Ionian Sea reflect the existence of multiple states in the Thermohaline circulation in the Eastern Mediterranean
- Aegean and Ionian Seas explicitly show a covariant behavior in the period 1987–2008
- The source of this covariant behavior relies on substantial zonal exchanges of salinity between the two basins

Correspondence to:
M. Reale
reale.marco82@gmail.com

Citation:
Reale, M., Salon, S., Crise, A., Farneti, R., Mosetti, R., & Sannino, G. (2017). Unexpected covariant behavior of the Aegean and Ionian Seas in the period 1987–2008 by means of a nondimensional sea surface height index. *Journal of Geophysical Research: Oceans*, *122*, 8020–8033. https://doi.org/10.1002/2017JC012983

Received 11 APR 2017
Accepted 5 SEP 2017
Accepted article online 14 SEP 2017
Published online 24 OCT 2017

Unexpected Covariant Behavior of the Aegean and Ionian Seas in the Period 1987–2008 by Means of a Nondimensional Sea Surface Height Index

M. Reale[1,2], S. Salon[2], A. Crise[2], R. Farneti[1], R. Mosetti[2], and G. Sannino[3]

[1]Earth System Physics Section, Abdus Salam International Centre for Theoretical Physics, Trieste, Italy, [2]Istituto Nazionale di Oceanografia e di Geofisica Sperimentale (OGS), Trieste, Italy, [3]Climate Modelling Laboratory, Italian National Agency for New Technologies-Energy -Sustainable Economic Development (ENEA), Roma, Italy

Abstract In this work, we use a set of recent multiyear simulations to develop a simplified sea surface height index (SSH). The index characterizes the dynamics of Ionian upper layer circulation and its links with sea surface height and salinity in the Southern Adriatic and Aegean Seas during the period 1987–2008. The analysis highlights a covariant behavior between Ionian Sea and Aegean Sea associated with a mutual zonal exchange of water masses with different salinity characteristics. Our analysis confirms that the variability observed in the period 1987–2008 in the upper layer circulation of the Ionian was driven by the salinity variability in the Southern Adriatic and Aegean Sea. This study supports and reinforces the hypothesis that two observed BiOS-like reversals reflect the existence of multiple equilibrium states in the Mediterranean Thermohaline circulation in the Eastern Mediterranean and that a complete characterization of observed variability needs to take into account a fully coupled Adriatic-Ionian-Aegean System.

1. Introduction

Recent observational and modeling studies suggested a primary role of the Aegean Sea in shaping the decadal variability of the upper layer circulation in the Ionian Sea, extending the concept of Adriatic-Ionian Bimodal Oscillating System (BiOS) (Gačić et al., 2010) to a coupled Adriatic-Ionian-Aegean system (Figure 1) (Amitai et al., 2016; Reale et al., 2016; Theocharis et al., 2014).

The Adriatic Sea (Figure 1) has an elongated shape (approximately 800 km long and 200 km wide) and is connected through the Otranto Strait (75 km wide and approximately 800 m deep) with the Ionian Sea. Historically, the Southern Adriatic has been identified as the main source of deep waters (also referred as Adriatic Deep Water (ADW); Manca et al., 2002; Querin et al., 2013, 2016) for the Eastern Mediterranean (EMED). ADW ranges approximately between 0.1 and 0.4 Sv (1Sv = 10^6 m^3 s^{-1}) with typical temperatures lower than 13.3°C, salinities higher than 38.68 and potential densities within the range of 29.17–29.18 kg m^{-3} (Gačić et al., 2002). ADW exits through the Otranto Strait oxygenating the deep layers of the Ionian Sea and EMED (Manca et al., 2002; Reale et al., 2016).

The Ionian Sea (Figure 1) is a crossroad for the Mediterranean Thermohaline Circulation (MTHC; Gačić et al., 2010). It is connected with the Western Mediterranean through the Sicily Channel, with the Levantine Basin through the Cretan Passage and with the Aegean Sea through the system of the West Cretan Straits (Figure 1). Usually its deep layers are filled with ADW, whereas its intermediate layers are influenced by warmer and saltier Levantine Intermediate Waters (LIW) moving westward. Ionian Sea surface layers are influenced by relatively fresher and colder Modified Atlantic Water (MAW) moving eastward (Gačić et al., 2010). Both LIW and MAW affect the density of ADW and deep waters potential formation (hereafter DWF, Gačić et al., 2010). The Aegean Sea (Figure 1) is a semienclosed basin of the EMED, connected with the Ionian Sea and Levantine basins through the eastern and western Straits of the Cretan Arc (Zervakis et al., 2004) and with the Black Sea through Bosporus and Dardanelles straits. Its bottom topography is characterized by an alternation of shelves and sills with deep basins (Zervakis et al., 2004). Aegean Sea circulation is characterized by a prevalent cyclonic pattern that increases the potential for open ocean convection and therefore DWF (Nittis et al., 2003).

During the Eastern Mediterranean Transient (EMT) event the main source of deep waters for the Eastern Mediterranean (EMDW) shifted from the Southern Adriatic to the Aegean Sea (Roether et al., 2007, among

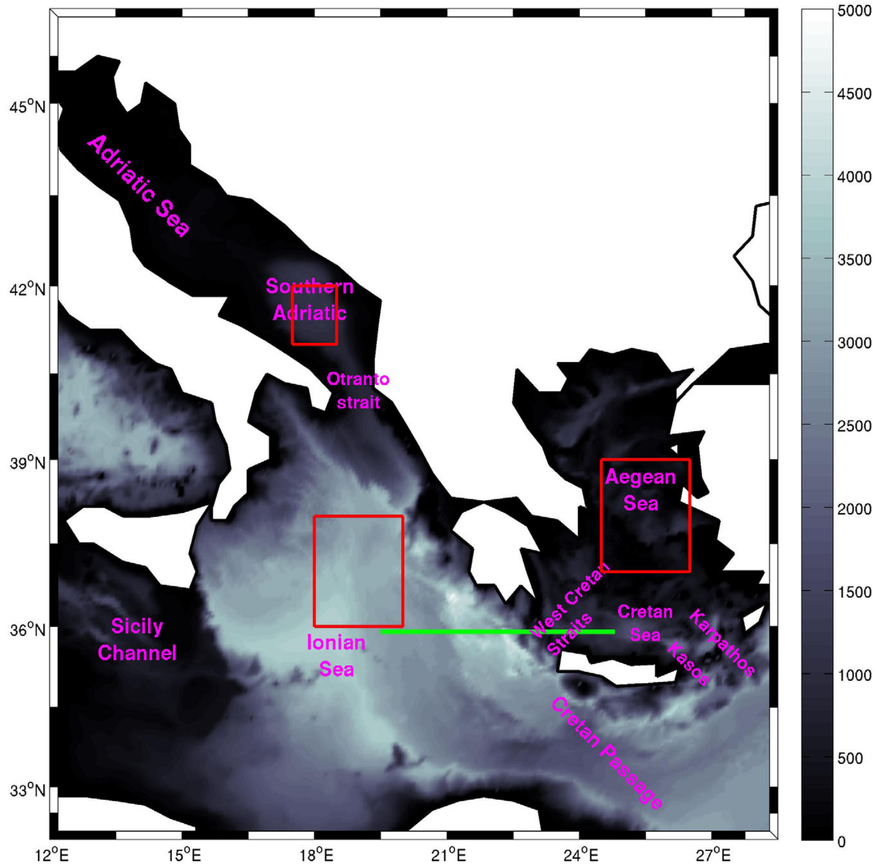

Figure 1. Bathymetry of Adriatic-Ionian-Aegean region (in m). Red squares mark the areas where the SSH index and Salinity have been computed. The green line represents the transect where the zonal transport of salinity has been computed.

the others). From 1987 and during 7 years, the deep layers of EMED received newly formed dense waters of Aegean origin, through the Kasos and Karpathos Strait (Figure 1), denser with respect to the Adriatic outflow, with temperature higher than 13.7°C, salinities higher than 38.8 and densities higher than 29.18 kg m^{-3} (Roether et al., 2007). This event peaked between mid-1992 and late 1994 delivering an average outflow of 3 Sv (Roether et al., 2007). This outflow rapidly spread across the Levantine basin and the Ionian by advection processes (partly retaining a cyclonic behavior rimming the periphery of the Ionian Sea) (Roether et al., 2007). The factors triggering the EMT have been identified in the intense winter cooling over the Aegean Sea during the winter 1987, 1992, and 1993 (Beuvier et al., 2010; Theocharis et al., 1999) that acted on top of a previous positive salinity anomaly between 1987 and 1991. The EMT event started to relax in 1995 (Theocharis et al., 2002) and the outflow almost stopped in 1998 (Klein et al., 2000). Presently, observations suggest that the main formation region of EMDW is back to the Adriatic (Klein et al., 2000), despite the fact that a recent reactivation of the Aegean Sea has been observed during 2007–2010 (Krokos et al., 2014).

The appearance of EMT has suggested the possibility of existence of multiple equilibrium states in the MHTC (Amitai et al., 2016; Ashkenazy et al., 2012). The transition between different states has been shown (through box models and idealized experiments) to be triggered by density differences between the Southern Adriatic and Aegean Seas and, in particular, has been associated with increasing (decreasing) salinity (temperature) over Aegean Sea (Amitai et al., 2016; Ashkenazy et al., 2012). Recent studies (Beuvier et al., 2010; Mihanović et al., 2015; Theocharis et al., 2014; Velaoras et al., 2015) identified three past events sharing with EMT the shift of deep waters formation from the Southern Adriatic to Aegean Sea but not the overall volume of deep waters formed: one at end of 1950s, one between 1962 and 1965 and one toward the end of 1970s.

In the last decade many studies based on remotely measured satellite or modeled Sea Surface Height (hereafter SSH, Bessieres et al., 2012; Gačić et al., 2010, 2014; Pinardi et al., 2015; Reale et al., 2016) pointed out the existence of two different circulation states in the Northern Ionian with a positive (negative) circulation state which corresponds to a positive (negative) SSH anomaly, i.e., anticyclonic (cyclonic) pattern. A first transition from anticyclonic to cyclonic mode was observed in 1997 and was attributed to the relaxation phase of EMT. An opposite transition has been observed between 2006 and 2011 (Gačić et al., 2010). An unexpected anticyclonic mode was observed in 2012 (Gačić et al., 2014) and it was attributed to extremely harsh conditions over the Adriatic Sea during the 2012 winter, which caused the formation of very dense ADW (Gačić et al., 2014). This transient phase ended in 2013 with the establishment of a new cyclonic state. The variability observed in the circulation, and hence in SSH, can clearly affect the salinity behavior of EMED, in the Sicily Channel (Gačić et al., 2011, 2013) and of salt, nutrients and mixed layer depth in the Adriatic Sea (Civitarese et al., 2010; Gačić et al., 2010; Mihanović et al., 2015; Reale et al., 2016).

Different mechanisms have been suggested as drivers of this variability: variability of wind stress curl over the basin (Pinardi et al., 2015), internal dynamics of the Adriatic-Ionian Seas system (Gačić et al., 2010), alternation between Southern Adriatic and Aegean Sea as the main DWF sites for EMED (Theocharis et al., 2014; Reale et al., 2016).

According to Gačić et al. (2010) Ionian and Adriatic Seas behave as a bimodal oscillating system (BiOS). When cyclonic conditions are present in the upper layer circulation of the Ionian Sea saltier LIW enter in the Adriatic leading to an increase of density in the ADW and of the potential for DWF. Later this newly formed ADW fills the Ionian bottom layers and induces a shallowing of isopycnal surfaces and the stretching of vorticity reversing the circulation from cyclonic to anticyclonic. In the upper layers, the anticyclonic circulation of the Ionian brings MAW into the Adriatic leading to a decrease of density in the ADW and of the potential for DWF. Finally this newly formed ADW fills the Ionian bottom layers and induces a deepening of isopycnal surfaces and the squeezing of vorticity reversing the circulation from anticyclonic to cyclonic.

Conversely, other authors (Krokos et al., 2014; Theocharis et al., 2014; Velaoras et al., 2014) suggest that the variability observed reflects an internal mechanism driving the alternation of the Adriatic Sea and Aegean Seas as main DWF sites for the EMED. When the Adriatic Sea is the main DWF site for the EMED, MAW is deflected northward in order to balance the outflow of ADW through the Otranto Strait. This deflection leads to a decrease of salinity in the Southern Adriatic and, thus, of the potential for DWF. At the same time, the recirculation of LIW in the Aegean Sea induces an increase of salinity in the basin and an increase of potential for DWF. A shift of DWF from the Southern Adriatic to the Aegean Sea eventually takes place. When Aegean Sea is the main DWF site for the EMED, MAW is deflected eastward in order to balance the outflow of Aegean deep waters through the Cretan Straits. This deflection together with an enhanced transport of LIW in the Southern Adriatic leads to an increase of salinity in the Southern Adriatic and of the potential for DWF. In the Aegean Sea, the transport of MAW induces a decrease of salinity in the basin and a decrease of potential for DWF. This results in the shift of DWF from the Aegean Sea to the Southern Adriatic. Under the above hypothesis, the anticyclonic (cyclonic) patterns observed in the Ionian Sea reflects the northward (southward) shift of the MAW in the Ionian Sea.

Recently Reale et al. (2016) has shown, through simplified process studies, that the variability observed in the period 1987–2008 can be explained only if the Aegean Sea dynamics is explicitly taken into account in the system. The transitions between the two circulation states have as main source of energy the conversion between Available Potential Energy (APE) and Kinetic Energy (KE) and is strictly linked to enhanced exchanges of APE between Aegean (Adriatic) Sea and Ionian Sea during the different circulation states in Ionian.

Thus, the observed reversals are consistent with the hypothesis of the existence of multiple equilibrium states in the MHTC (Amitai et al., 2016; Ashkenazy et al., 2012; Theocharis et al., 2014) and then they can be explained only taking into account a fully coupled Adriatic-Ionian-Aegean system (Crisciani & Mosetti, 2016; Reale et al., 2016).

Here we first define a simplified nondimensional index for the SSH to characterize the interactions between Ionian, Adriatic, and Aegean Sea during the period 1987–2008. Then we show the existence of a covariant behavior between the Ionian and Aegean Seas strictly linked to zonal exchanges of water masses with different salinity characteristics. We also confirm the feedback mechanism involving salinity variation between Southern Adriatic and Aegean Seas and the circulation in the Ionian Sea during the period 1987–2008. Finally we show how the variability observed reflects the existence of multiple equilibrium states in the Adriatic-Ionian-Aegean system.

2. Materials and Methods

This study aims at analyzing the dynamics of the Adriatic-Ionian-Aegean Sea system using a multimodel approach. The advantages of using a multimodel approach in the Mediterranean region have been shown in the analysis of heat and salt budget (Harzallah et al., 2016; Llasses et al., 2016), but also in analysis of atmospheric circulation over the area (Flaounas et al., 2016). These studies have shown that a multimodel approach is able to describe the main features and mechanisms driving the atmosphere-ocean circulation over the Mediterranean region (Ruti et al., 2014). A multimodel analysis will thus provide us with a more robust characterization of the variability in the Ionian Sea.

In the next sections, we describe the numerical simulations used in this study (for more details about the single simulation please refer to the references reported in Table 1) and outline the procedure followed to derive the nondimensional index applied to the SSH.

2.1. Adriatic-Ionian System (AISys) Experiments

AISys experiments (Reale et al., 2016; Table 1) cover the period 1987–2008 and have been designed as a process study for the analysis of the variability of upper layer circulation in the Ionian Sea in response to wind forcing and thermohaline lateral fluxes.

AISys experiments have been performed using the MITgcm (Adcroft et al., 1997; Marshall et al., 1997a, 1997b), a primitive equation model implemented over Adriatic-Ionian System. The domain of integration consists of the Southern Adriatic and Ionian Sea. The spatial resolution is 0.125° with 36 vertical levels. The model is forced with 3 hourly wind fields from RegCM4 simulations (Giorgi et al., 2012) for the MedCordex domain (Ruti et al., 2014). Current speed from MyOcean data set (Oddo et al., 2009) and temperature and salinity from the NEMOMED8 experiment (Beuvier et al., 2010) are used as lateral boundary conditions. In the case of temperature and salinity boundary conditions an averaged profile was computed for each month for the period 1987–2008 and applied over each boundary (Sicily Channel, West Cretan Straits, and Cretan Passage).

AISys experiments represent a process study (Reale et al., 2016) and some forcings (e.g., heat fluxes) have not been derived from preexisting data sets but have been artificially created in order to recreate the DWF over Southern Adriatic, to compensate the absence of the DWF over Northern Adriatic and to ensure a realistic outflow/volume of ADW through the Otranto strait. Evaporation, precipitation and runoff fluxes were not taken into account during the experiments. Initial conditions for both temperature and salinity have been derived from the data of German cruises in the area in the 1987 (Roether et al., 2007). These vertical profiles were applied to the entire domain and used in 20 year long spin-up experiment. The resulting final temperature and salinity 3-D fields were used as initial conditions for the following experiments. Initial velocities are null over the domain.

Table 1
Main Characteristics of the Simulation Data Sets Selected for This Work

Model	Period	Horizontal and vertical resolution	Initial conditions	Boundary conditions	References
AISys	1987–2008	1/8° 36 levels	Modified Roether Conditions	Artificial Heat Fluxes, MyOcean, RegCM4, NEMOMED8	Reale et al. (2016)
NEMOMED8	1961–2008	1/8° 43 levels	MedAtlas-II	Arpera	Beuvier et al. (2010) Hermann et al. (2010)
MedMIT12	1979–2012	1/12° 75 levels	MedAtlas-II	Aldera	Harzallah et al. (2016) Llasses et al. (2016)
Copernicus	1955–2014	1/16° 72 levels	SeaDataNet	AMIP	Oddo et al. (2009) Adani et al. (2011); Fratianni et al. (2015) E.U. Copernicus Marine Service Information (http://marine.copernicus.eu/services-portfolio/access-to-products/?option=com_csw&view=details&product_id=MEDSEA_REANALYSIS_PHYS_006_009.)

2.2. Nemomed8

NEMOMED8 model is the configuration for the Mediterranean area of the NEMO ocean model (Table 1, Beuvier et al., 2010; Herrmann et al., 2010). It covers the whole Mediterranean and a buffer zone including a portion of the Atlantic Ocean. The Black Sea is parameterized as a river runoff in the Aegean Sea. The experiment used in this study covers the period 1961–2008 and has been used before for the investigation of the factors triggering the EMT (see Beuvier et al., 2010) and the formation of deep waters in the Western Mediterranean (Herrmann et al., 2010). The spatial resolution is 0.125° with 43 vertical levels. The model uses boundary conditions from ARPERA daily mean fields of momentum, freshwater and heat flux (Beuvier et al., 2010). ARPERA derives from the dynamical downscaling of ERA40 (Simmons & Gibson, 2000) by the regional climate model ARPEGE (Déqué & Piedelievre, 1995). Initial conditions are derived by Medatlas II climatologies for the 1960s and the model was initially run until a spin up is reached. The resulting 3-D outputs were employed as final initial conditions for the experiment.

2.3. MedMIT12

MedMIT12 (Harzallah et al., 2016; Llasses et al., 2016) is the MITgcm (Table 1, Adcroft et al., 1997) adapted to the Mediterranean region and implemented at a horizontal resolution of 1/12° with 75 vertical levels. The model covers the whole Mediterranean Sea plus a buffer zone including a small portion of the near Atlantic Ocean. The Black Sea is parameterized as a surface freshwater flux applied at the mouth of the Strait of Dardanelles. The atmospheric fields used to force the simulation come from the regional downscaling of ERA-interim reanalysis called ALDERA, a 12 km run performed with ALADIN52_v1 and ERA-interim as lateral boundary conditions (Hermann et al., 2011), covering the years 1979–2013. The ocean model is forced by net freshwater flux (including river runoff) and by net heat flux. The MedMIT12 experiment has been first run with a relaxation both to ERA-interim values of Sea Surface Temperature, and to climatological values of Sea Surface Salinity with time relaxation constants of 2 days and 1.8 days, respectively. The salinity relaxation term so obtained has been then converted into a climatological flux correction added to the forcing freshwater flux. The initial conditions have been chosen as the mean state of October 1979, according to the MedAtlas data set, and no spin up has been performed.

2.4. Copernicus

The reanalysis produced by the Copernicus Marine Environment Monitoring Services (originally derived from the MyOcean projects, Oddo et al. (2009) and Adani et al. (2011), corresponding to the Version 2 product MEDSEA_REANALYSIS_PHYS_006_009; see main features in Table 1 and further details in Fratianni et al. (2015)) are based on the NEMO-OPA 3.2 and 3.4 models. NEMO has been implemented in the Mediterranean Sea at 1/16° horizontal resolution and 72 vertical levels (Oddo et al., 2009) and it is nested in the Atlantic. The model is forced by momentum, heat, and freshwater fluxes interactively computed by bulk formulae adapted to the Mediterranean case, using AMIP data (Cherchi & Navarra, 2007) with a correction applied to the heat flux. The Dardanelles inflow is parameterized as a river, with the climatological net inflow rates from Kourafalou and Barbopoulos (2003). The model uses the OceanVar three-dimensional variational assimilation scheme (Dobricic & Pinardi, 2008) assimilating in-situ temperature and salinity vertical profiles from CTDs, XBTs, MBTs, bottles, ARGO, and altimeter satellite measurements. Initial conditions correspond to a gridded climatology for temperature and salinity computed from in-situ data sampled contained in SeaDataNet.

2.5. Derivation of the Nondimensional Index for the SSH

The use of a nondimensional SSH index for characterizing the dynamics and the reversals in the Ionian Sea (combined with another index for the eddy KE) has been already introduced in Bessieres et al. (2012). In the present work, we adopt a simplified version of this index based only on the SSH term to study the dynamics of the Ionian, Southern Adriatic and Aegean Seas upper layers. The use of a nondimensional index is further justified since we compared this quantity among different models with different resolution, parametrizations and forcings.

The computation of the nondimensional SSH index has been carried out as follows:

- the original monthly SSH data have had the seasonal cycle removed for the period covered by each simulation (this was introduced to avoid any influence on the SSH variability due to seasonal or steric effect which are substantial in data sets where sea level data are assimilated as in Copernicus; P. Cipollini (personal communication, 2016)

- the resulting monthly anomalies have been then used to compute an annual SSH anomaly (SSHa) for each year of simulation over a selected area
- the nondimensional SSH index is defined as:

$$SSHi = \left(SSHa_{j=1,nyear} - SSHMa\right) / std_{SSHa} \quad (1)$$

where SSHMa is the mean of SSHa over all the simulated years for each model and std_{SSHa} is its standard deviation. The procedure adopted for the computation of the index maintains the sign and variability of the original field and thus can be adopted to study the variability of the sea surface. This is demonstrated in Figure 2 where we show the comparison between the area-averaged Absolute Dynamical Topography field (hereafter ADT) over the Ionian (a), Southern Adriatic (b), and Aegean Sea (c) and SSHi computed using ADT data. By definition, ADT is equal to the sum of Sea Level anomaly (SLA) and Mean Dynamic Topography (MDT). The MDT is the part of Mean Sea Surface Height due to permanent currents, so that MDT corresponds to the Mean SSH minus Geoid (SSALTO/DUACS Users Handbook, 2016, Available at http://www.aviso.altimetry.fr/en/data/product-information/aviso-user-handbooks.html). The regional Mediterranean ADT product is computed using a specific regional MDT (Mediterranean Sea only). The data are on regular spatial grid of 1/8° and covers the period 1993–2013. ADT data have been extensively used in previous studies (Bessieres et al., 2012; Borzelli et al., 2009) to describe the reversals in the Ionian upper layer circulation.

The targeted regions for the computation of SSHi (Figure 1) have coordinates 18°E–20°E and 36°N–38°N (Ionian), 17.5°E–18.5°E, and 41°N–42°N (Southern Adriatic) and 24.5°E–26.5°E and 37°N–39°N (Aegean). The Ionian area has been chosen through a previous analysis (not shown) of SLA anomaly maps which shows, in the period 1993–2013, a change in terms of sign of Northern Ionian Gyre (NIG) already pointed out in previous studies (e.g., Gačić et al., 2010; Pinardi et al., 2015) and clearly visible in Figure 2. The area in the Southern Adriatic has been already adopted in previous studies (Gačić et al., 2010; Reale et al., 2016) to point out

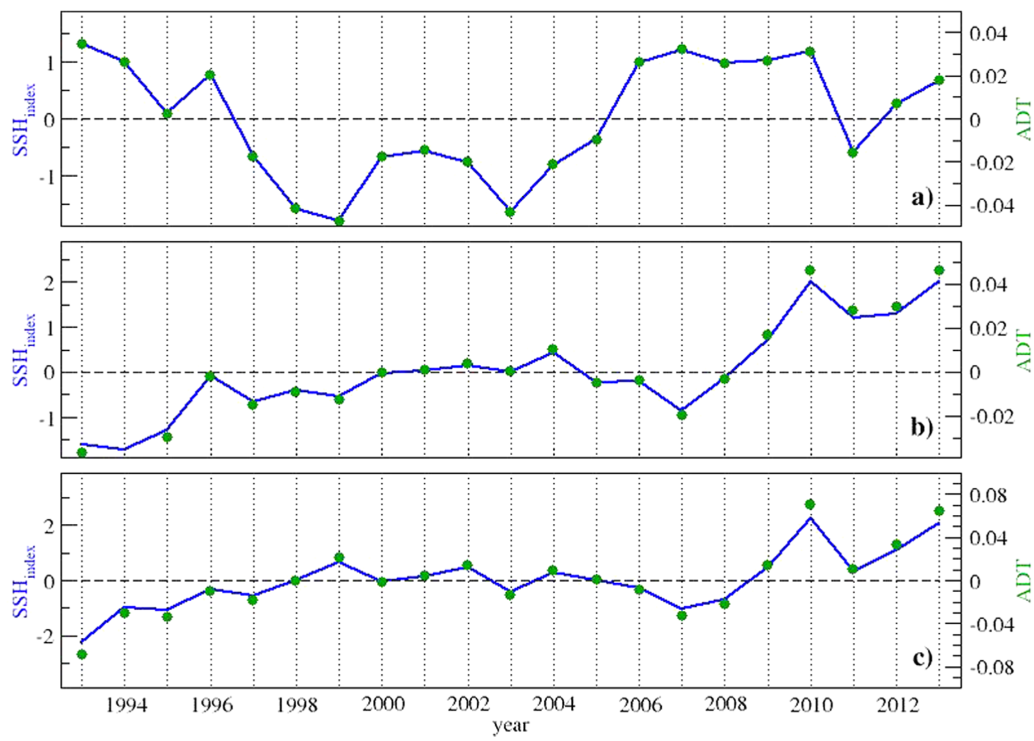

Figure 2. ADT (green dots, in m) and SSHi (blue) in the period 1993–2013 computed in the (a) Ionian, (b) Southern Adriatic, and (c) Aegean Sea.

the possible influence of the Ionian circulation on the intermediate layers of Southern Adriatic. Finally the area in the Aegean Sea has been chosen according to Nittis et al. (2003) as the primary site for the DWF in the Aegean Sea. Figure 2a shows that SSHi is able to capture the two states of circulation in the Northern Ionian as also clearly visible in ADT data. In particular, both SSHi and ADT time series show the positive (anticyclonic) circulation pattern up to 1997, a negative (cyclonic) circulation pattern up to 2005, a new positive pattern until 2011 and a change between positive and negative pattern between 2012 and 2013. All these patterns in the Ionian Sea have been already identified in previous studies (e.g., Bessieres et al., 2012; Borzelli et al., 2009; Gačić et al., 2010, 2014; Pinardi et al., 2015; Reale et al., 2016; Theocharis et al., 2014). Also in Southern Adriatic (b) and Aegean Sea (c) the SSHi maintains the sign and variability of ADT data, hence the simplified index here defined can be used to describe the variability of circulation in the three regions. The SSHi has been computed for each available simulation. As in previous studies (Bessieres et al., 2012), the identification of the two circulation patterns in the Ionian is based only on the sign of the SSHi not on its value.

3. Results

Figure 3 shows the SSHi computed in Ionian (a), Southern Adriatic (b), and Aegean Sea (c). The analyses cover the period 1987–2008 to allow the overlapping among the available simulation data sets given that the Copernicus data set is the only simulation available until 2014. Figure 3a shows that in the Ionian after 1993 all the simulations present a good agreement with the SSHi computed using ADT (hereafter ADT SSHi). The SSHi derived from each multiyear simulations and their mean have a positive peak in 1993–1994 corresponding to the maximum of the EMT. This is related to the presence of an anticyclonic pattern in the Ionian as widely reported in the scientific literature (see Reale et al., 2016, and the references therein).

After 1997 all multiyear simulations and their mean show a reversal in the Ionian circulation with a negative pattern lasting until 2005. After 2005, the SSHi calculated for all the models and their mean shows the reversal to the positive pattern. The interannual-decadal variability of SSHi in the Ionian is very well in line with the phenomenology sketched in the introduction. Despite the differences among models in reproducing

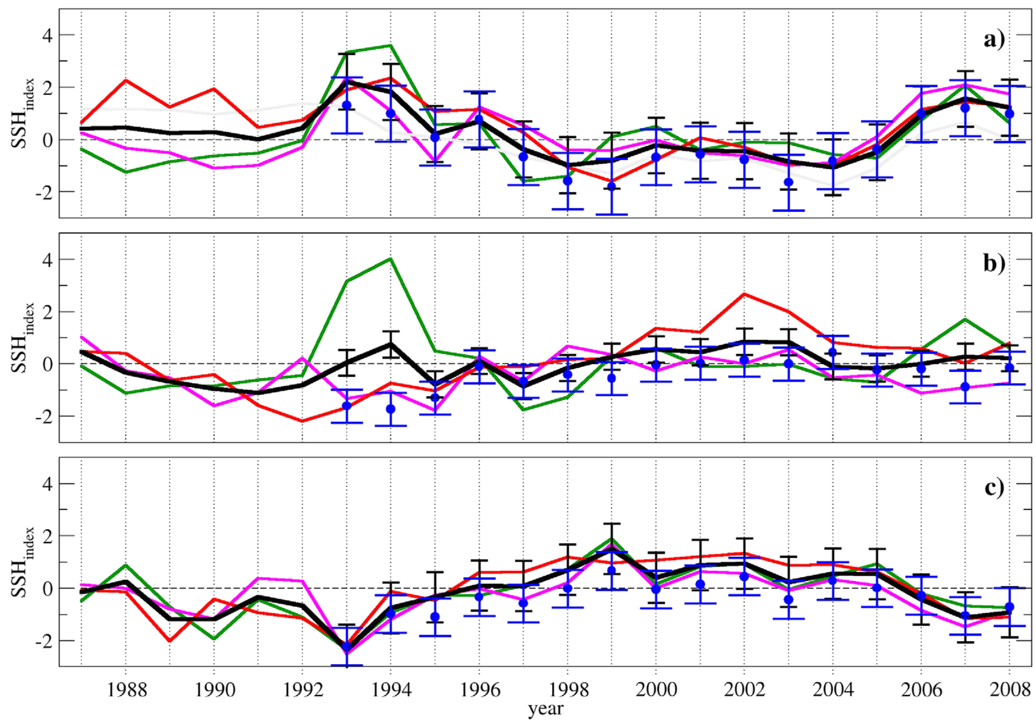

Figure 3. Annual-mean SSHi during the period 1987–2008 computed in the (a) Ionian, (b) Southern Adriatic, and (c) Aegean Sea: based on ADT (blue dots), NEMOMED8 (green), Copernicus (red), MedMIT12 (magenta), AISys (gray, only for the Ionian Sea) data and the mean of all simulations (black). The standard deviation has been computed for the mean of all simulations and for the ADT SSHi and reported in the figure as vertical error bar.

Table 2
Lag Correlation (LC) and Coefficients of Linear Regressions Between Different Indexes

Linear correlation/regression	Coefficients	Time lag for max LC
Linear Regressions Between the Ionian, Southern Adriatic, and Aegean SSHi		
Ionian-Aegean	LC = −0.82 R^2 = 0.66 a = −0.83	0
Ionian-Southern Adriatic	LC = −0.44 R^2 = 0.17 a = −0.61	SA(−2)/IO
Southern Adriatic-Aegean	LC = 0.50 R^2 = 0.26 a = 0.36	SA/AE(−2)
Linear Regressions Between the Ionian SSHi Southern Adriatic and Aegean SALi (0–100 m)		
Ionian-Aegean (0–100 m)	LC = 0.71 R^2 = 0.54 a = 0.68	0
Ionian-Southern Adriatic (0–100 m)	LC = 0.70 R^2 = 0.50 a = 0.88	SA(−2)/IO
Southern Adriatic-Aegean (0–100 m)	LC = 0.80 R^2 = 0.50 a = 0.80	SA(−3)/AE
Linear Regressions Between the Ionian SSHi, Southern Adriatic and Aegean SALi (200–800 m)		
Ionian-Aegean (200–800 m)	LC = 0.72 R^2 = 0.60 a = 0.69	IO/AE(+1)
Ionian-Southern Adriatic (200–800 m)	LC = 0.60 R^2=0.40 a = 0.77, b = 0.28	SA(−2)/IO
Southern Adriatic-Aegean (200–800 m)	LC = −0.60 R^2 = 0.36 a = −0.55	SA/AE(−4)

Note. The Salinity index is calculated in the upper layer (0–100 m) and in the intermediate layer (200–800 m). Only values significant at 90% of confidence are reported. R^2 is the regression coefficient, a and b are the coefficient of linear regression $y = ax + b$ (reported only when significant). The time lag where LC is maximum is expressed in years.

the SSHi value, they all agree in showing the existence of two circulation patterns in the area. In particular, their mean reproduces quite well the behavior of ADT SSHi. It is worthwhile to mention that, despite the spread among the models, the mean is able to capture the anticyclonic pattern in the Northern Ionian in the period 1987–1988, which has been discussed in previous studies (Demirov & Pinardi, 2002).

The same good agreement between the ADT SSHi, the multiyear simulations and their mean can be observed in the Aegean Sea (Figure 3c). Here all time-series show a progressive increase in the Aegean SSHi after 1993 and a progressive decrease after 2000. Moreover, the mean Ionian SSHi and Aegean SSHi show a well-defined antiphase tendency. Conversely, a similar good agreement between model data and ADT SSHi is not observed in the case of Southern Adriatic (Figure 3b), where the spread among the models is high, showing positive and negative phases in the same year. Further, neither of the mean fits well the variability observed in ADT SSHi. These differences may probably be related to the small area chosen for the Southern Adriatic, the different resolutions of the models, the lower signal-to-noise ration of altimeter data in coast-bounded regions, or all of them. Hereafter, the mean of all the simulations will be used in the statistical analysis.

Table 2 (upper part) shows that the linear time-lag correlation (LC) of linear regression between Southern Adriatic and Ionian SSHi reaches its maximum in correspondence of a 2 years delay but this result needs to be considered with caution owing the poor correlation. The same consideration holds when considering the linear regression between Southern Adriatic and Aegean SSHi. In this case, the Southern Adriatic SSHi is weakly correlated with the Aegean SSHi, with a delay of 2 years. The coefficient of both linear regressions can explain only a small amount of variability (Table 2). Conversely the Ionian-Aegean LC exhibits a significant anti-correlation with an R^2 of 0.66 reaching surprisingly its top a 0 lag. This means that the Ionian and the Aegean SSHis variations can be considered synchronous.

Figure 4 shows the mean annual salinity computed between 0–100 m (upper layer) and 200–800 m (intermediate layer) in the Southern Adriatic (Figures 4a and 4c) and Aegean (Figures 4b and 4d) for the model simulations and their mean (AISys has been excluded as it does not include the Aegean region in its domain).The depths of the two layers have been chosen as they represent the location of MAW and LIW. In Southern Adriatic (Figures 4a and 4c) both NEMOMED8 and MedMIT12 show alternate phases of increase and decrease of the salinity in the upper/intermediate layer. This behavior is not present in Copernicus where a slight decrease (increase) trend in salinity can be seen. The variability highlighted by the mean was also observed in the experimental data and previous studies (Gačić et al., 2010; Reale et al., 2016; Theocharis et al., 2014).

In order to correlate the salinity in both basins with the circulation pattern and vice versa in Ionian, a salinity index (SALi) for both Southern Adriatic and Aegean has been computed using equation (1). Table 2 (intermediate and lower part) shows the lag correlation and the linear regression coefficient between the Ionian

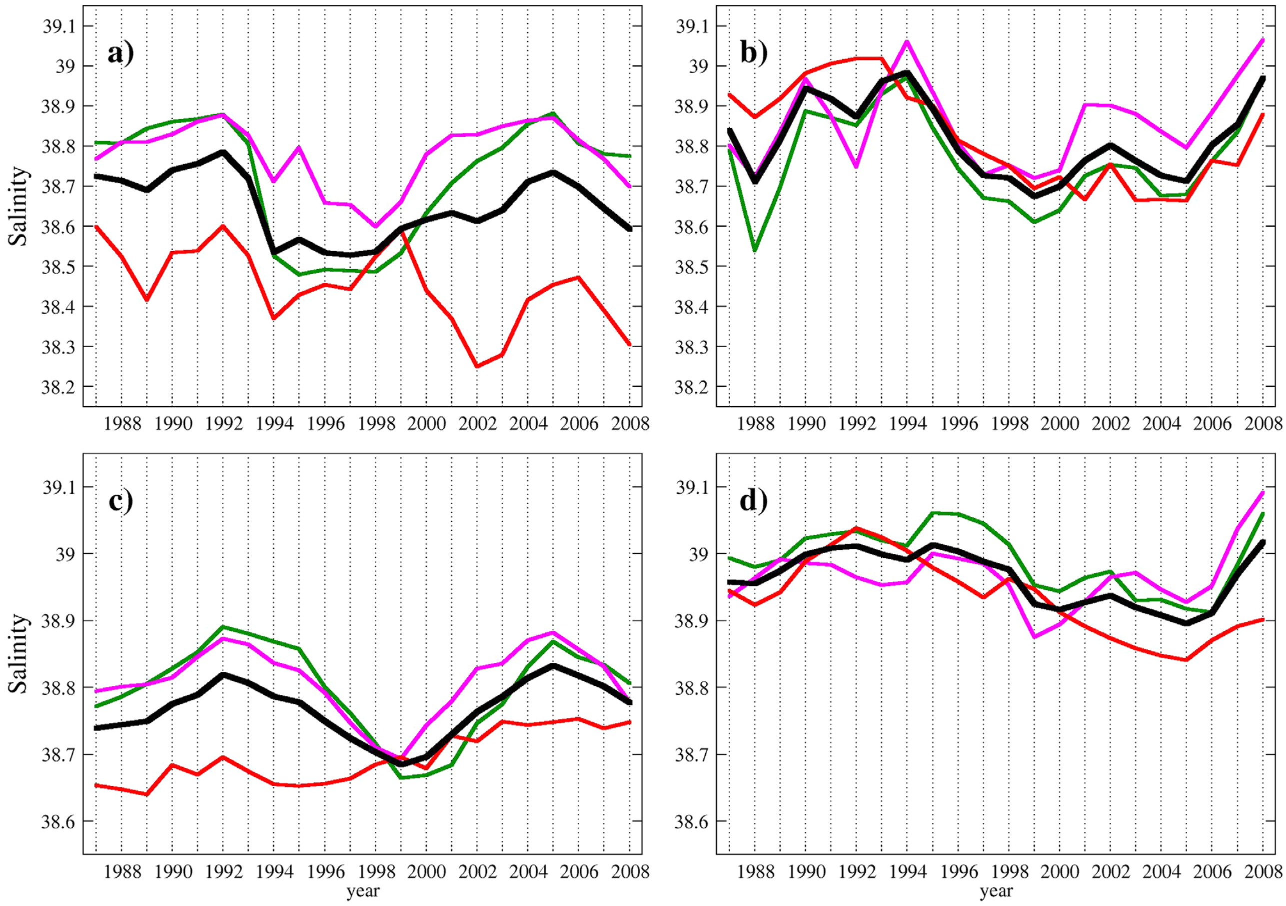

Figure 4. (a and c) Salinity (in psu) in the Southern Adriatic and (b and d) Aegean Sea (a and b) between 0–100 m and (c and d) 200–800 m according to NEMOMED8 (green), Copernicus (red), and MedMIT12 (magenta) and their mean (black).

SSHi and Southern Adriatic and Aegean SALi, respectively, in the upper and intermediate layer. Surprisingly, in the upper layer of the Aegean the SALi and the Ionian SSHi are positively correlated with a zero time lag (as found, but with opposite sign, for the correspondent SSHis). The Southern Adriatic SAL_i is also positively correlated with the Ionian SSHi (Aegean SALi) with a time lag of two (three) years. All regressions show a R^2 greater than or equal to 0.50 and so they explain at least 50% of the observed variability (Table 2). The highest value is observed between the Ionian SSHi and the Aegean SALi (Table 2).

For the intermediate layer (Table 2), the Aegean SALi is correlated with the Ionian SSHi with a one year delay. Southern Adriatic SALi and Ionian SSHi maintain the same time lag as in the upper layer. Southern Adriatic SALi and Aegean SALi are negatively correlated with a time lag of four year. The latter confirms the results of previous studies that highlight the opposite behavior of the salinity in the two basins (see Bensi et al., 2016; Krokos et al., 2014; Theocharis et al., 2014; Velaoras et al., 2014) and the importance of the Aegean in influencing the salinity of the intermediate layer in the Southern Adriatic (Amitai et al., 2016). The Salinity/SSH based indexes in the upper layer in both Southern Adriatic and Aegean have the same time lag (Table 2) with the Ionian SSHi, suggesting that variations in upper layer salinity and SSH are connected.

The observed variability in salinity affects also the maximum mixed layer depth behavior in February (MLD, de Boyer Montegut et al., 2004) in both basins (Figures 5a and 5b). The increase (decrease) in salinity in both basins corresponds to an increase (decrease) in MLD (Figures 5a and 5b) which is affected in late winter by the open ocean convection and is related to an increase in the DWF intensity (Nittis et al., 2003). This could explain the enhanced negative pattern in the observed Aegean SSHi. In fact, as clearly shown in Figure 3c, Aegean SSHi shows two relative minima: one in 1993 corresponding to the EMT peak (e.g., Roether et al., 2007), and one in 2007 corresponding to the reactivation of the Aegean as dense water formation site

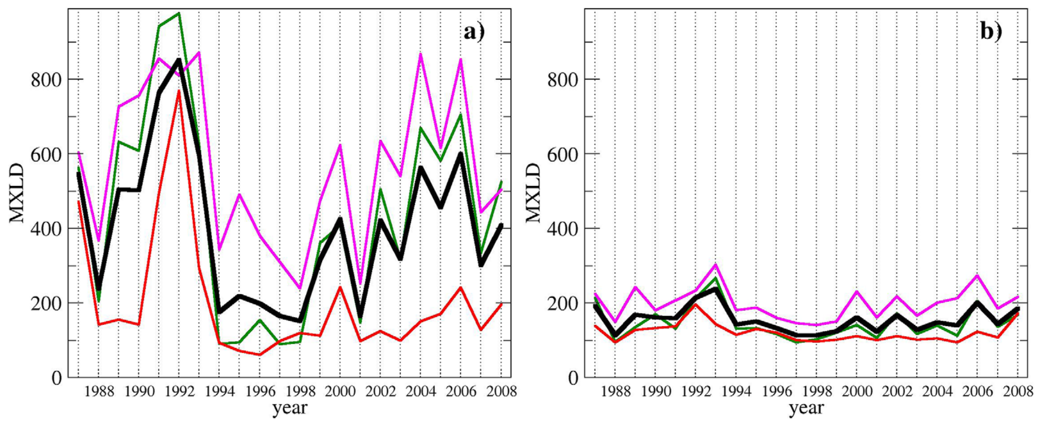

Figure 5. MLD (in m) in (a) Southern Adriatic and (b) Aegean Sea according to NEMOMED8 (green), Copernicus (red), and MedMIT12 (magenta) and their mean (black).

(Krokos et al., 2014). The MLD computed in the Aegean (Figure 5b) shows two relative maxima: one in 1993 and one in 2006 depicting a large open ocean convection in the area and thus DWF. Conversely, in the same years, the MLD in the Southern Adriatic (Figure 5a) was characterized by a sudden decrease (after a period of sharp increasing) indicating a reduced DWF (Amitai et al., 2016; Dunić et al., 2016; Theocharis et al., 2014).

Straddling the end of the 1980s and the beginning of the 1990s, during a positive Ionian SSHi, the northward shift of MAW in the Ionian leads to a sharp increase of salinity in the upper layer of the Aegean and the year after in its intermediate layer. The progressive increase of salinity in both upper and intermediate layer enhances the cyclonic circulation at the center of the Aegean and leads to a decrease in the Aegean SSHi (which corresponds to the increase of MLD). This reflects on the DWF shift from the Southern Adriatic to the Aegean (e.g., EMT, Roether et al., 2007; Theocharis et al., 2014). When the difference between the Ionian and Aegean SSHi is such as to accelerate MAW toward the Aegean, a decrease in salinity takes place in the Aegean, leading to an increase of SSHi (and a decrease of the MLD) in the area (Theocharis et al., 2014). Meanwhile, after the mid-1990s, due to the lower input of MAW, the Southern Adriatic begins to become saltier at the surface and then in its intermediate layers due to an enhanced advection of LIW (see Gačić et al., 2010; Reale et al., 2016) leading to a increase of MLD (despite a sudden observed decrease in 2001 which was associated with very mild conditions over the area in February (Sellschopp & Alvarez, 2003)) and affecting the Ionian SSHi. This results in a shift of DWF from the Aegean to the Southern Adriatic, as already observed in Klein et al. (2000) and Theocharis et al. (2014). While the MAW begins to shift northward, with a new reversal after 2005, the Aegean begins to become saltier and the cycle starts again (Theocharis et al., 2014).

These final results support the idea that the reversals observed in the period 1987–2008 reflect the existence of multiple equilibrium states in MTHC in the EMED and that Adriatic-Ionian-Aegean Sea system behaves like a coupled system (Amitai et al., 2016; Ashkenazy et al., 2012; Crisciani & Mosetti, 2016; Reale et al., 2016; Theocharis et al., 2014).

From another point of view these results explain the reasons why we used the term “unexpected” and “surprisingly” in relation to the covariant behavior of Aegean and Ionian Seas, highlighted in the previous statistical analysis. This is clear observing Figures 6a,b,c, where the monthly mean zonal transport of salinity between Aegean and Ionian Seas in the period 1987–2008 is shown (centered on 36°N and computed between 19.5°E and 24.5°E, green line in Figure 1). During the positive phase of Ionian SSHi the zonal flow of salinity is absent or mainly oriented from the center of the Ionian toward the Cretan Sea, filling, as stated before, the upper layer of the Aegean with fresher MAW water and leading to the decrease of salinity in the Aegean. During a negative SSHi the direction of the flow reverses, filling the upper layer of the Ionian with saltier Aegean water, further decreasing the salinity in the Aegean itself and increasing the strength of cyclonic circulation in the Ionian. Hence, the source of the covariant behavior observed between the Ionian and Aegean SSHi and between the Ionian SSHi and the Aegean SALi is associated with an advective signal of monthly temporal scale, as shown in the Hovmoeller diagrams in Figure 6.

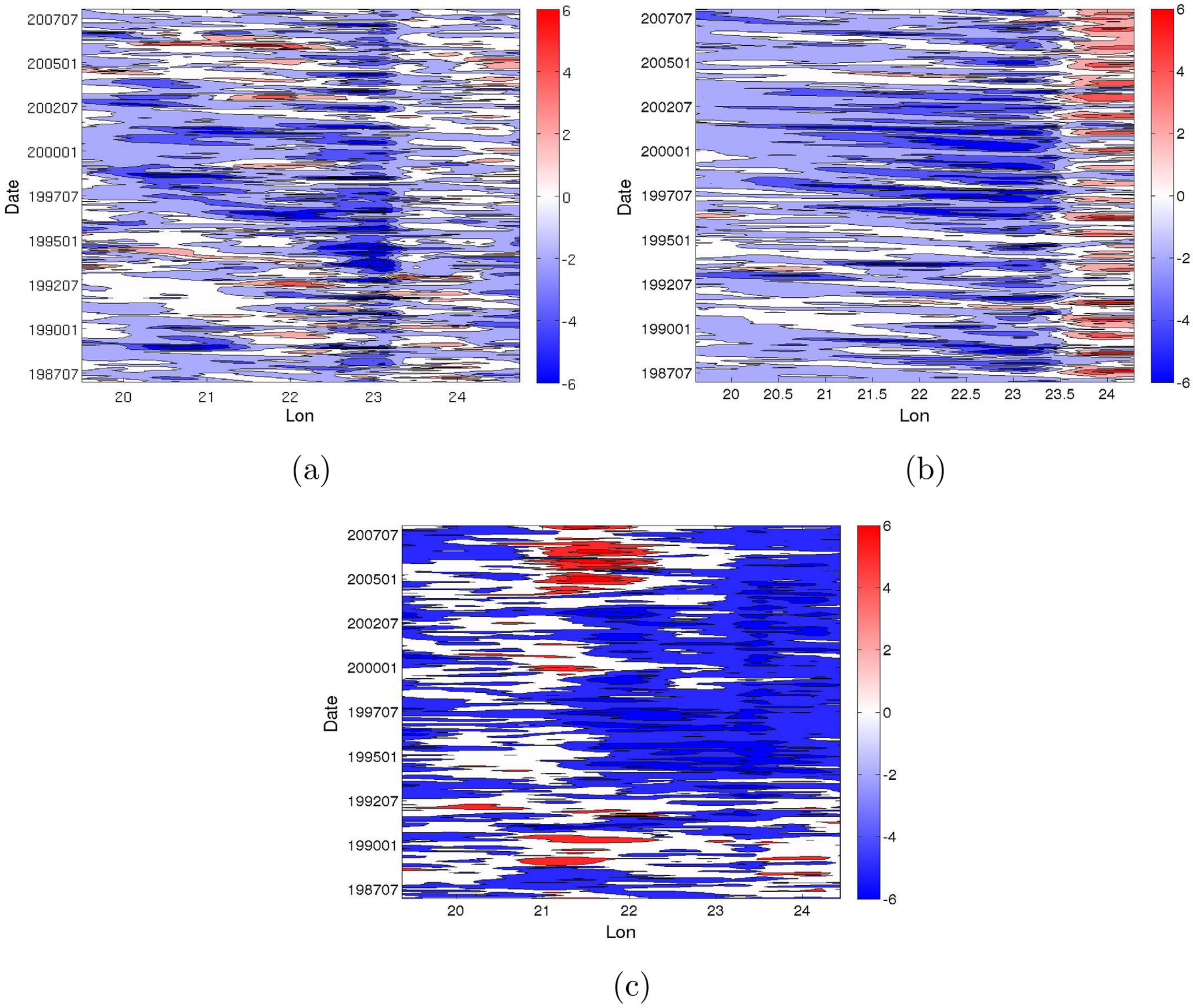

Figure 6. Hovmoeller diagrams of zonal flux of salinity (in psu ms^{-1}), monthly-mean values for the top 50 m, computed between 19.5°E and 24.5°E and 36°N in (a) NEMOMED8, (b) MedMIT12, and (c) Copernicus for the period 1987–2008.

The existence of this advective signal and the related time scale has been suggested in previous studies supported by experimental data (Krokos et al., 2014; Velaoras et al., 2014) and numerical experiments (Reale et al., 2016; Theocharis et al., 2014). In this work, the advective signal is confirmed by the validation of SSHi against ADT data and by the use of a multimodel approach. On the other hand the interaction between the Southern Adriatic and the Ionian does not appear to take place on the same time scale and with same advective signal. The Ionian SSHi exhibits a delay of 2 years with respect the salinity in the Southern Adriatic, and the reasons for that will be addressed in a future study.

Finally, comparing Figure 3 with Figure 4 (by means of a scatter plot, not shown here) it appears that a salinity upper layer value above (below) 38.8 in the Aegean characterizes the positive (negative) SSHi in the Ionian, whereas for the intermediate layer the two different patterns in the Ionian hold for a value of salinity above (below) 38.95. In the case of the Southern Adriatic, on average, for the upper layer salinity a value above (below) 38.7 in the Southern Adriatic can be linked with a time delay of 2 years to a possible positive (negative) pattern in the Ionian, while for the intermediate layer this can be speculated to exist for a value of salinity above (below) 38.75.

4. Conclusions

In this paper, a simplified index for SSH in the Ionian Sea has been introduced and used to describe the reversals of the Ionian Sea upper layer circulation that took place in the region between 1987 and 2008. The comparison with satellite data and results from the scientific literature has allowed us to test the ability of the Ionian SSHi to capture the dynamics of the Ionian. As shown in previous studies, a cyclonic pattern persists between 1997 and 2005, whereas an anticyclonic pattern is found between 1987–1996 and 2006–2011. The multimodel approach has shown the potential to overcome the spread among the models and to reconstruct the variability of the upper layer in the Ionian Sea, as described in previous studies. This is particularly true in the case of the 1987–1988 reversal (Demirov & Pinardi, 2002), which has been well captured by multimodel mean but not by all the singular models. This 1987–1988 reversal has been attributed to atmospheric forcing through wind stress curl changes (Demirov & Pinaridi, 2002). It is likely that the different forcing spatial resolution used in each model can explain the observed spread.

The comparison of the Ionian SSHi with the SALi in the Aegean and Southern Adriatic has shown the following:

1. The Aegean and the Ionian Seas explicitly show a covariant behavior in the period 1987–2008. In particular, Aegean upper layer salinity covaries in the time with the Ionian SSHi. Salinity in the Aegean intermediate layer shows a delay of one year with respect to the Ionian SSHi.
2. The source of the covariant behavior of the two basins is an advective signal involving the salinity and acting on a monthly scale in both directions.
3. The existence of this advective signal has been suggested by previous numerical and experimental studies (Krokos et al., 2014; Reale et al., 2016; Theocharis et al., 2014). Here we have confirmed the signal by validating the SSHi against ADT data and through a multimodel approach.
4. The shift of MAW toward the Aegean Sea is followed by a salinity and MLD increase in the Southern Adriatic. This induces an increase of sea level difference between the center of the Ionian and Southern Adriatic, and thus a progressive shift northward of MAW toward the Southern Adriatic. The time scale associated is larger than the one observed between the Ionian and the Aegean Seas.
5. Positive (negative) patterns in the Ionian Sea are observed in together with upper layer salinity above (below) 38.8 in the Aegean Sea.
6. For the Southern Adriatic, a value of upper layer salinity above (below) 38.7 could be used to forecast Ionian reversal two years in advance.
7. The comparison of the SSHi with ADT data and Salinity data in the period 1987–2008 has confirmed the presence of multiple equilibrium states in the MHTC of the EMED (Amitai et al., 2016; Ashkenazy et al., 2012).
8. BiOS-like observations during the period 1987–2008 reflect the switching between the two possible deep water sources for the EMED (Reale et al., 2016; Theocharis et al., 2014).

The influences of external forcings on this system, in particular wind and surface fluxes, and their effect on the temporal scale of reversals are however still to be analyzed. Further experiments based on a new generation of coupled models are in preparation in order to analyze more in depth these effects and to evaluate them from an energetic point of view. Some experiments will be specifically oriented toward the analysis of the time delay between the Ionian and the Southern Adriatic.

Acknowledgments
The authors acknowledge S. Somot (samuel.somot@meteo.fr), F. Sevault, and Meteo-France/CNRM, for running and providing upon request the NEMOMED8 data simulation. This study has been conducted using E.U. Copernicus Marine Service Information: the authors acknowledge the European Copernicus Marine Environmental Monitoring Services for their open access data policy (http://marine.copernicus.eu/). The ADT altimeter data used in this paper were produced by SSALTO/DUACS and distributed by AVISO with support from CNES (www.aviso.altimetry.fr/duacs/). Copernicus data are available on http://marine.copernicus.eu/while MedMIT12 and NEMOMED8 data are available upon registration on www.medcordex.eu. AISys data are available on http://clima-dods.ictp.it/Users/rfarneti/AISysexp/. The authors are very grateful to D. Velaoras for his useful comments and suggestions on the preliminary version of this work. M. Reale acknowledges the support for this work of OGS and CINECA under the HPC-TRES program award number 2015-07.

References

Adani, M., Dobricic, S., & Pinardi, N. (2011). Quality assessment of a 1985–2007 Mediterranean Sea reanalysis. *Journal of Atmospheric and Oceanic Technology*, *28*(4), 569–589.

Adcroft, A., Hill, C., & Marshall, J. (1997). The representation of topography by shaved cells in a height coordinate model. *Monthly Weather Review*, *125*(9), 2293–2315.

Amitai, Y., Ashkenazy, Y., Gildor, H. (2016). Multiple equilibria and overturning variability of the Aegean-Adriatic Seas. *Global and Planetary Change*, *151*, 49–59. https://doi.org/10.1016/j.gloplacha.2016.05.004

Ashkenazy, Y., Stone, P., & Malanotte-Rizzoli, P. (2012). Box modeling of the Eastern Mediterranean sea. *Physica A: Statistical Mechanics and its Applications*, *391*(4), 1519–1531. https://doi.org/10.1016/j.physa.2011.08.026

Bensi, M., Velaoras, D., Meccia L. V., & Cardin V. (2016). Effects of the Eastern Mediterranean Sea circulation on the thermohaline properties as recorded by fixed deep-ocean observatories. *Deep Sea Research Part I: Oceanographic Research Papers*, *112*, 1–13. https://doi.org/10.1016/j.dsr.2016.02.015

Bessieres, L., Rio, M., Dufau, C., Boone, C., & Pujol, M. (2012). Ocean state indicators from MyOcean altimeter products. *Ocean Science*, *9*(3), 545–560. https://doi.org/10.5194/osd-9-2081-2012

Beuvier, J., Sevault, F., Herrmann, M., Kontoyiannis, H., Ludwig, W., Rixen, M., . . . Somot S. (2010). Modeling the Mediterranean Sea interannual variability during 1961–2000: Focus on the Eastern Mediterranean transient. *Journal of Geophysical Research*, *115*, C08017. https://doi.org/10.1029/2009JC005950
Borzelli, G. L. E., Gačić, M., Cardin, V., & Civitarese, G. (2009). Eastern Mediterranean transient and reversal of the Ionian Sea circulation. *Geophysical Research Letters*, *36*, L15108. https://doi.org/10.1029/2009GL039261
Cherchi, A., & Navarra, A. (2007). Sensitivity of the Asian summer monsoon to the horizontal resolution: Differences between AMIP-type and coupled model experiments. *Climate Dynamics*, *28*(2), 273–290. https://doi.org/10.1007/s00382-006-0183-z
Civitarese, G., Gačić, M., Lipizer, M., & Eusebi Borzelli, G. L. (2010). On the impact of the Bimodal Oscillating System (BiOS) on the biogeochemistry and biology of the Adriatic and Ionian Seas (Eastern Mediterranean). *Biogeosciences*, *7*, 3987–3997. https://doi.org/10.5194/bg-7-3987-2010
Crisciani, F., & Mosetti, R. (2016). Is the bimodal oscillating Adriatic-Ionian circulation a stochastic resonance. *Bollettino di Geofisica Teorica ed Applicata*, *57*(3), 275–285.
de Boyer Montegut, C., Madec, G., Fischer, A. S., Lazar, A., & Iudicone, D. (2004). Mixed layer depth over the global ocean: An examination of profile data and a profile-based climatology. *Journal of Geophysical Research*, *109*, C12003. https://doi.org/10.1029/2004JC002378
Demirov, E., & Pinardi, N. (2002). Simulation of the Mediterranean Sea circulation from 1979 to 1993: Part I. The interannual variability. *Journal of Marine Systems*, *33–34*, 23–50. https://doi.org/10.1016/S0924-7963(02)00051-9
Déqué, M., & Piedelievre, J. (1995). High resolution climate simulation over Europe. *Climate Dynamics*, *11*, 321–339.
Dobricic, S., & Pinardi, N. (2008). An oceanographic three-dimensional variational data assimilation scheme. *Ocean Modelling*, *22*(3–4), 89–105. https://doi.org/10.1016/j.ocemod.2008.01.004
Dunić, N., Vilibić, I., Šepić, J., Somot, S., & Sevault, F. (2016). Climate modelling of the dense water formation and BiOS-induced variability in the Adriatic Sea: The first results. *Climate Dynamics*, 1–26.
Flaounas, E., Kelemen, F., Wernli, H., Gaertner, M. A., Reale, M., Sanchez, E., . . . Conte, D. (2016). Assessment of an ensemble of ocean-atmosphere coupled and uncoupled regional climate models to reproduce the climatology of Mediterranean cyclones. *Climate Dynamics*, 1–18. https://doi.org/10.1007/s00382-016-3398-7
Fratianni, C., Simoncelli, S., Pinardi, N., Cherchi, A., Grandi, A., & Dobricic, S. (2015). Mediterranean RR 1955-2015 (Version 1). (Data set). *Copernicus Monitoring Environment Marine Service (CMEMS)*. https://doi.org/10.25423/MEDSEA_REANALYSIS_PHY_006_009
Gačić, M., Borzelli, G. L. E., Civitarese, G., Cardin, V., & Yari, S. (2010). Can internal processes sustain reversals of the ocean upper circulation? The Ionian Sea example. *Geophysical Research Letters*, *37*, L09608. https://doi.org/10.1029/2010GL043216
Gačić, M., Civitarese, G., Eusebi Borzelli, G. L., Kovacevic, V., Poulain, P.-M., Theocharis, A., . . . Zarokanellos, N. (2011). On the relationship between the decadal oscillations of the northern Ionian Sea and the salinity distributions in the eastern Mediterranean. *Journal of Geophysical Research*, *116*, C12002. https://doi.org/10.1029/2011JC007280
Gačić, M., Civitarese, G., Kovacevic, V., Ursella, L., Bensi, M., Menna, M., . . . Pizzi, C. (2014). Extreme winter 2012 in the Adriatic: An example of climatic effect on the BiOS rhythm. *Ocean Science*, *10*, 513–522. https://doi.org/10.5194/os-10-513-2014
Gačić, M., Lascaratos, A., Manca, B., & Mantziafou, A. (2002). Adriatic deep water and interaction with the Eastern Mediterranean Sea. In B. Cushman-Roisin, M. Gačić, P.-M. Poulain, & A. Artegiani (Eds.), *Physical oceanography of the Adriatic Sea. Past, present and future* (Chapter 4, pp. 111–142). Netherlands: Springer.
Gačić, M., Schroeder, K., Civitarese, G., Cosoli, S., Vetrano, A., & Eusebi Borzelli, G. L. (2013). Salinity in the Sicily Channel corroborates the role of the Adriatic-Ionian Bimodal Oscillating System (BiOS) in shaping the decadal variability of the Mediterranean overturning circulation. *Ocean Science*, *9*(1), 83–90.
Giorgi, F., Coppola, E., Solmon, F., Mariotti, L., Sylla, M. B., Bi, X., . . . Brankovic C. (2012). RegCM4: Model description and preliminary tests over multiple CORDEX domains. *Climate Research*, *52*, 7–29.
Harzallah, A., Jordà, G., Dubois, C., Sannino, G., Carillo, A., Li, L., . . . Akhtar, N. (2016). Long term evolution of heat budget in the Mediterranean Sea from Med-CORDEX forced and coupled simulations. *Climate Dynamics*, 1–21. https://doi.org/10.1007/s00382-016-3363-5
Herrmann, M., Sevault, F., Beuvier, J., & Somot, S. (2010). What induced the exceptional 2005 convection event in the northwestern Mediterranean basin? Answers from a modeling study. *Journal of Geophysical Research*, *115*, C12051. https://doi.org/10.1029/2010JC006162
Herrmann, M., Somot, S., Calmanti, S., Dubois, C., & Sevault, F. (2011). Representation of spatial and temporal variability of daily wind speed and of intense wind events over the Mediterranean Sea using dynamical downscaling: impact of the regional climate model configuration. *Natural Hazards and Earth System Sciences*, *11*, 1983–2001.
Klein, B., Roether, W., Civitarese, G., Gačić, M., Manca, B. B., & Ribera D'alcala, M. (2000). Is the Adriatic returning to dominate the production of Eastern Mediterranean Deep Water?. *Geophysical Research Letters*, *27*(20), 3377–3380.
Kourafalou, V. H., & Barbopoulos, K. (2003). High resolution simulations on the North Aegean Sea seasonal circulation. *Annales Geophysicae*, *21*(1 Part 2), 251–265.
Krokos, G., Velaoras, D., Korres, G., Perivoliotis, L., & Theocharis, A. (2014). On the continuous functioning of an internal mechanism that drives the Eastern Mediterranean thermohaline circulation: The recent activation of the Aegean Sea as a dense water source area. *Journal of Marine System*, *129*, 484–489. https://doi.org/10.1016/j.jmarsys.2013.10.002
Llasses, J., Jordà, G., Gomis, D., Adloff, F., Macías, D., Harzallah, A., . . . Sannino, G. (2016). Heat and salt redistribution within the Mediterranean Sea in the Med-CORDEX model ensemble. *Climate Dynamics*, 1–25. https://doi.org/10.1007/s00382-016-3242-0
Manca, B. B., Kovacevic, V., Gačić, M., & Viezzoli, D. (2002). Dense water formation in the Southern Adriatic sea and spreading into the Ionian Sea in the period 1997–1999. *Journal of Marine Systems*, *33–34*, 133–154.
Marshall, J., Adcroft, A., Hill, C., Perelman, L., & Heisey, C. (1997a). A finite-volume, incompressible Navier Stokes model for studies of the ocean on parallel computers. *Journal of Geophysical Research*, *102*(C3), 5753–5766.
Marshall, J., Hill, C., Perelman, L., Heisey, C., & Adcroft, A. (1997b). Hydrostatic, quasi-hydrostatic and nonhydrostatic ocean modeling. *Journal of Geophysical Research*, *102*(C3), 5733–5752.
Mihanović, H., Vilibić, I., Dunić, N., & Sepić, J. (2015). Mapping of decadal middle Adriatic oceanographic variability and its relation to the BiOS regime. *Journal of Geophysical Research: Oceans*, *120*, 5615–5630. https://doi.org/10.1002/2015JC010725
Nittis, K., Lascaratos, A., & Theocharis, A. (2003). Dense water formation in the Aegean Sea: Numerical simulations during the Eastern Mediterranean Transient. *Journal of Geophysical Research*, *108*(C9), 8120. https://doi.org/10.1029/2002JC001352
Oddo, P., Adani, M., Pinardi, N., Fratianni, C., Tonani, M., & Pettenuzzo, D. (2009). A nested Atlantic-Mediterranean Sea general circulation model for operational forecasting. *Ocean Science*, *5*, 461–473. https://doi.org/10.5194/os-5-461-2009
Pinardi, N., Zavatarelli, M., Adani, M., Coppini, G., Fratianni, C., Oddo, P., . . . Bonaduce, A. (2015). Mediterranean Sea large-scale low-frequency ocean variability and water mass formation rates from 1987 to 2007: A retrospective analysis. *Progress in Oceanography*, *132*, 318–332. https://doi.org/10.1016/j.pocean.2013.11.003

Querin, S., Bensi, M., Cardin, V., Solidoro, C., Bacer, S., Mariotti, L., & Stel, F. (2016). Saw-tooth modulation of the deep water thermohaline properties in the southern Adriatic Sea. *Journal of Geophysical Research: Oceans*, *121*, 4585–4600. https://doi.org/10.1002/2015JC011522

Querin, S., Cossarini, G., & Solidoro, C. (2013). Simulating the formation and fate of dense water in a midlatitude marginal sea during normal and warm winter conditions. *Journal of Geophysical Research: Oceans*, *118*, 885-900. https://doi.org/10.1002/jgrc.20092

Reale, M., Crise, A., Farneti, R., & Mosetti, R. (2016). A process study of the Adriatic-Ionian System baroclinic dynamics. *Journal of Geophysical Research: Oceans*, *121*, 5872–5887. https://.doi.org/10.1002/2016JC011763

Roether, W., Klein, B., Manca, B., Theocharis, A., & Kioroglou, S. (2007). Transient Eastern Mediterranean deep waters in response to the massive dense-water output of the Aegean Sea in the 1990s. *Progress in Oceanography*, *74*, 540–571.

Ruti, P., Somot, S., Giorgi, F., Dubois, C., Flaounas, E., Obermann, A., . . . Vervatis, V. (2014). MED-CORDEX initiative for Mediterranean Climate studies. *Bulletin of the American Meteorological Society*, *97*, 1187–1208.

Sellschopp, J., & Alvarez, A. (2003). Dense low-salinity outflow from the Adriatic Sea under mild (2001) and strong (1999) winter conditions. *Journal of Geophysical Research*, *108*(C9), 8104. https://doi.org/10.1029/2002JC001562

Simmons, A. J., & Gibson, J. K. (2000). *The ERA-40 Project plan* (ERA-40 Project Rep. Ser. No. 1, 63 p.). Reading, UK: ECMWF.

Theocharis, A., Klein, B., Nittis, K., & Roether, W. (2002). Evolution and status of the East Mediterranean transient (1997–1999). *Journal of Marine Systems*, *33*, 91–116.

Theocharis, A., Krokos, G., Velaoras, D., & Korres, G. (2014). An internal mechanism driving the alternation of the Eastern Mediterranean dense/deep water sources. In G. L. E. Borzelli, M. Gačić, P. Lionello, & P. Malanotte-Rizzoli (Eds.), *The Mediterranean sea: Temporal variability and spatial patterns*. AGU Geophysical Monograph Series (Vol. 202, pp. 113–137). Oxford: John Wiley. https://doi.org/10.1002/9781118847572.ch8

Theocharis, A., Nittis, K., Kontoyiannis, H., Papageorgiou, E., & Balopoulos, E. (1999). Climatic changes in the Aegean Sea influence the Eastern Mediterranean thermohaline circulation. *Geophysical Research Letters*, *26*(11), 1617–1620.

Velaoras, D., Krokos, G., Nittis, K., & Theocharis, A. (2014). Dense intermediate water outflow from the Cretan Sea: A salinity driven, recurrent phenomenon, connected to thermohaline circulation changes. *Journal of Geophysical Research*, *119*, 4797–4820. https://doi.org/10.1002/2014JC009937

Velaoras, D., Krokos, G., & Theocharis, A. (2015). Recurrent intrusions of transitional waters of Eastern Mediterranean origin in the Cretan Sea as a tracer of Aegean Sea dense water formation events. *Progress in Oceanography*, *135*, 113–124.

Zervakis, V., Georgopolous, D., Karageorgis, A., & Theocharis, A. (2004). On the response of the Aegean sea to climatic variability: A review. *International Journal of Climatology*, *24*, 1845–1858.